Int. J. Heat Mass Transfer. Vol. 19, pp. 1337–1339. Pergamon Press 1976. Printed in Great Britain

SHORTER COMMUNICATION

MASS-TRANSFER EXPERIMENTS ON SECONDARY-FLOW VORTICES IN A CORRUGATED WALL CHANNEL

LEONARDO GOLDSTEIN, JR. and E. M. SPARROW
Department of Mechanical Engineering, University of Minnesota, Minneapolis, Minnesota, U.S.A.

(*Received* 3 *January* 1976)

NOMENCLATURE

- H, channel height, Fig. 1;
- L, streamwise length, Fig. 1;
- l, width of spanwise measurement zone, Fig. 2;
- $m(z)$, local rate of mass transfer per unit area;
- $\overline{m(z)}$, spanwise average mass-transfer rate, equation (1);
- R_1, inner radius of curved circular arc channel;
- R_2, outer radius of curved circular arc channel;
- Re, Reynolds number, $2H\bar{u}/\nu$;
- $\bar{u}$, mean velocity;
- W, overall spanwise width, Fig. 2;
- x, streamwise coordinate;
- z, spanwise coordinate;
- λ, wavelength of spanwise mass-transfer variation;
- ν, kinematic viscosity.

INTRODUCTION

WHEN a flow is bounded by a surface having longitudinal curvature, secondary motions in the form of longitudinal vortices may occur. The onset of such secondary motions is due to the centrifugal instability of the main flow. The analysis of the instability process for laminar boundary-layer flow along a concave wall was first performed by Görtler, with subsequent significant contributions by Hämmerlin and by Smith (see [1] and [2] for a summary). Experimental evidence of the existence of longitudinal vortices in curved boundary-layer flows has been provided by several investigators (for instance [3–6]), but the conditions marking the onset of the vortex motion have, apparently, not been identified experimentally.

The occurrence of longitudinal vortices superposed on a laminar main flow has also been studied for curved channels whose bounding walls are concentric circular arcs. The initial analysis of the centrifugal instability which marks the onset of vortex motion was performed by Dean [7] for the case where the spacing between the walls is small compared with the radius of curvature. The narrow gap assumption was retained by several subsequent investigators [8–12], but was lifted in [13] to accommodate channels having arbitrary spacing between the walls. Flow visualization techniques were employed by Brewster and co-workers [11] to determine the conditions at the onset of the vortex motion.

Channel flows with non-planar bounding walls are encountered frequently in advanced heat exchange devices (e.g. in compact heat exchangers). Furthermore, because of the small dimensions characteristic of such devices, the flow is often in the laminar regime. Typically, these channel configurations are highly complex and differ appreciably from the simple circular arc channels whose laminar instability characteristics have been investigated in the past.

A class of channel configurations that frequently recurs in practice is characterized by walls that are wavy or corrugated in the main flow direction. Owing to the streamline curvature induced by the shape of the wall, centrifugal forces are activated. The direction of the centrifugal forces depends upon whether the streamline curvature is convex or concave. Since the walls of a wavy or corrugated channel impose periodic concave and convex curvature on the streamlines, the direction of the centrifugal force will vary along the length of the channel.

The present research was undertaken to investigate experimentally the onset of secondary-flow vortex motions in a corrugated wall channel. The flow field behavior will be inferred from detailed local measurements of the surface mass transfer via the naphthalene sublimation technique. The absence or presence of a periodic spanwise variation of the local mass-transfer rates enabled detection of the conditions marking the onset of vortex motion. The detailed nature of the measurements also facilitated the determination of the wavelength of the secondary flow. Whereas sublimation of naphthalene (or para-dichlorobenzene) has been used previously as a qualitative visualization tool to illustrate the presence of secondary-flow vortices [6, 14], it was not employed to obtain quantitative information on the onset and the character of the vortex motion.

The work reported here is part of a study of the transfer characteristics of laminar, transitional, and low-Reynolds-number turbulent flows in a corrugated wall heat-transfer channel [15, 16].

THE EXPERIMENTS

The experimental apparatus, measurement technique, and data reduction procedures will be outlined here only in general terms, with more detailed information available in [15] and [16]. A schematic side view of the test section showing the corrugated wall naphthalene plates in place is presented in Fig. 1. Each of the corrugated walls consists of four facets, respectively sloped at an angle of about 21° relative to the horizontal. The selection of the facet slope as well as of the dimensions H and L, respectively equal to 1.65 and 18.5 mm, was guided by those of an actual heat exchange device.

To suppress extraneous mass transfer, all surfaces of each naphthalene plate were covered with a pressure-sensitive tape, except for the corrugated surface that bounds the flow channel. During the data runs, air from the temperature-

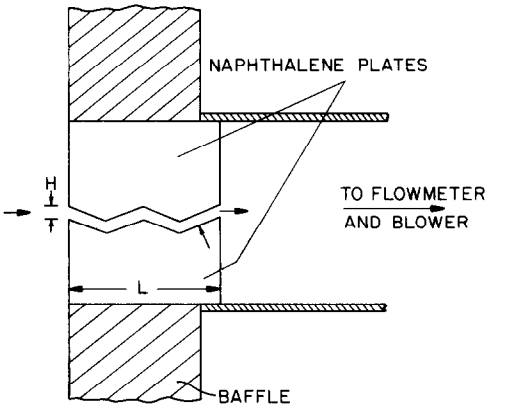

FIG. 1. Schematic side view of the test section.

controlled laboratory ($\sim 20^{\circ}$C) was drawn through the test section and ultimately exhausted to the outdoors at the roof of the building.

The naphthalene plates were cast in specially designed and fabricated molds. The surfaces produced by the casting process possessed a high degree of smoothness and flatness so that no subsequent machining was necessary. For each data run, a new pair of naphthalene plates, cast from never-used reagent-grade naphthalene, were employed.

Surface contour measurements were made both immediately before and after a data run with the aid of a sensitive dial gage having a smallest scale division of 0.00005 in (~ 0.001 mm). For the contour measurements, a naphthalene plate was positioned on a movable coordinate table which could be traversed in two directions in the horizontal plane. The measurement procedure is most conveniently described with the aid of Fig. 2, which is a plan view of the corrugated wall channel. At a fixed streamwise station x, contour measurements were performed by traversing the stylus of the dial gage in the spanwise (i.e. cross stream) direction z.

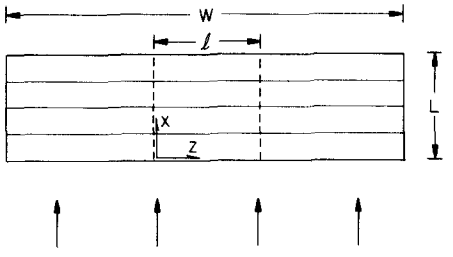

FIG. 2. Schematic plan view of the corrugated wall channel.

The spanwise width within which the measurements were made is denoted by l. Readings were taken at every 0.2 mm along the z direction. With $l = 19$ mm, each spanwise traverse encompassed 96 data points. The overall spanwise width W was 70.1 mm.

The local differences between the before and after surface contour measurements were employed, in conjunction with the duration time of a data run, to determine the local mass-transfer rates. Corrections were applied to account for extraneous natural convection sublimation, which occurred during the period of surface contour measurement and during the assembly of the test section, and for uncertainties in positioning on the coordinate table [15].

At any given streamwise location, the measurements and subsequent data reduction yielded the spanwise distribution of the local rate of mass transfer per unit area $m(z)$. For each $m(z)$ distribution, a spanwise average value was determined from

$$\overline{m(z)} = \frac{1}{l}\int_0^l m(z)\,dz \qquad (1)$$

and this, in turn, enabled evaluation of a normalized spanwise distribution $m(z)/\overline{m(z)}$.

RESULTS AND DISCUSSION

Preliminary qualitative experiments were performed to determine whether and at what Reynolds numbers secondary-flow vortices existed. These experiments revealed that such motions did exist at certain Reynolds numbers and, furthermore, that the presence of the vortices was much more strongly manifested on certain facets of the corrugated wall. These findings served to guide the final quantitative experiments, both with respect to the Reynolds number range and to the streamwise locations at which mass-transfer measurements were made.

The second and fourth facets of the lower wall of the channel (both of which are windward facets) were generally most strongly influenced by the secondary motions. Therefore, to establish the Reynolds number marking the onset

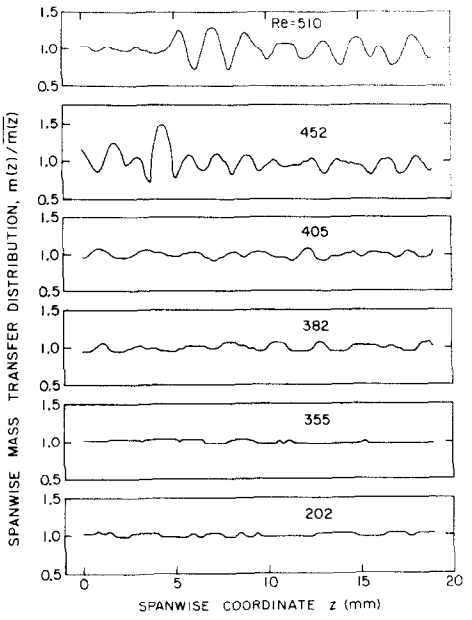

FIG. 3. Spanwise mass-transfer distributions showing the evolution of secondary-flow vortices with increasing Reynolds number.

of secondary flow, attention will be focused on a streamwise location on one of these facets, and a station on the fourth facet (identified by the arrow in Fig. 1) has been chosen for this purpose. At that station, the spanwise mass-transfer distributions will be examined as a function of the Reynolds number. The presence or absence of spanwise variations will be used to discriminate as to the presence or absence of secondary-flow vortices. Graphs showing the evolution of spanwise mass transfer distributions at several other streamwise locations are available in [15].

The stability characteristics will be deduced with the aid of Fig. 3. In the figure, normalized spanwise mass-transfer distributions $m(z)/\overline{m(z)}$ are plotted as a function of z for each of several Reynolds numbers in the range from 200 to 500. The motivation for employing normalized distributions is to give the results for all Reynolds numbers a common baseline (i.e. a mean value of unity) and thereby facilitate identification of departures from the baseline due to secondary flow.

The Reynolds number Re is defined using the equivalent diameter for a parallel plate channel $D_e = 2H$, so that

$$Re = 2H\bar{u}/\nu \qquad (2)$$

where $\bar{u}$ is the mean velocity of the main flow. Each of the curves has its own ordinate scale, which is centered about 1.0. As noted earlier, each curve represents 96 discrete data points.

Inspection of the figure clearly indicates an evolution of secondary-flow vortices with increasing Reynolds number. In the range between 200 and 350, the spanwise distributions are effectively flat, as witnessed by the curves of Fig. 3 as well as those of the preliminary experiments. The slight departures from complete flatness are indicative of the resolving power of the instrumentation, which is about 0.00005 in. The spanwise distribution for $Re = 382$ contains the first indications of a patterned variation. Therefore, the onset of the secondary flow, as manifested by its effect on surface transfer processes, occurs in the range between $Re = 355$ and 382. With increasing Reynolds number, the strength of the secondary flow increases, and the periodic nature of the spanwise variation becomes more clear. The wavelength of the periodic variation is about 2 mm.

It is of interest to compare the foregoing findings with the predictions of stability theory. Such an undertaking is

handicapped because the stability of the flow in a corrugated wall channel has not yet been analyzed. Although there are distinct differences, the nearest flow configuration for which stability predictions exist appears to be the curved channel whose bounding walls are concentric circles (inner and outer radii R_1 and R_2, respectively). Those predictions will be compared with the present results for the corrugated wall channel, but with the recognition that such a comparison cannot be strictly quantitative.

For the wavelength λ, narrow-gap stability theory gives the result

$$\lambda = (2\pi/3.96)H. \tag{3}$$

The accounting of a finite gap size [13] brings about a slight increase in the constant so that, for instance, when $R_1/R_2 = 0.5$, the constant is 4.32 instead of 3.96. If the channel height $H = 1.65$ mm of the experiment is introduced, equation (3) gives $\lambda = 2.62$ mm, whereas if the constant 4.32 is used in the denominator, then $\lambda = 2.40$ cm. From their experiments on circular arc channels, Brewster and coworkers [11] found a correlation of their wavelength results using a constant of 4.9. With this constant and $H = 1.65$ mm, equation (3) yields $\lambda = 2.11$ cm.

The wavelength $\lambda \simeq 2$ mm observed in the present experiments is not significantly different from the λ values discussed in the last paragraph. In view of the fact that the corrugated wall channel and the circular arc channel are characterized by significantly different main flows, the just-cited comparison suggests that the wavelength may not be very sensitive to the details of the channel main flow.

For the Reynolds number marking the onset of instability in a circular arc channel, the narrow-gap theory gives

$$Re = 71.9\sqrt{(R_1/H)} \tag{4}$$

where R_1 is the radius of the inner bounding wall. The instability Reynolds number predicted by the finite-gap analysis can be substantially larger than that of equation (4), depending on the radius ratio R_1/R_2.

If consideration is given to using equation (4) for predicting an instability Reynolds number for comparison with the present results, a fundamental difficulty is encountered in identifying a numerical value for R_1. The walls of a plane-faceted corrugated channel do not have a radius of curvature. In the absence of a better approach, the authors have determined a value of R_1 as that of a circle which is tangent to the mid-points of two adjacent facets. This procedure gives $R_1 = 6.4$ mm. Upon introduction of this value into equation (4) along with $H = 1.65$ mm and with a multiplying factor of 1.18 to account for the finite-gap correction [13] corresponding to $H/R_1 = (1.65)/(6.4)$, there is obtained $Re = 167$. As noted earlier, the present experiments yielded an instability Reynolds number of about 370. No definite significance can be attached to the difference between these Reynolds number values because equation (4) is not directly applicable to corrugated wall channels. Perhaps the most interesting outcome of the comparison is that the application of equation (4), in conjunction with an estimate of R_1, can yield reasonable predictions of the instability Reynolds numbers for other than circular arc channels.

As a final remark, it may be noted that the evolution of a strong and regularly patterned spanwise variation, which is evidenced by Fig. 3, was not observed on the leeward facets. This is believed due to the influence of flow separation [15, 16].

Acknowledgement—Scholarship support from the Brazilian National Council of Research (CNPq) and from Pontificia Universidade Catolica do Rio de Janeiro extended to Leonardo Goldstein, Jr. is gratefully appreciated. The research was supported by the National Science Foundation under Grant ENG-7503221.

REFERENCES

1. L. Rosenhead, *Laminar Boundary Layers*, pp. 502–505. Oxford, London (1963).
2. H. Schlichting, *Boundary Layer Theory*, pp. 504–508. McGraw-Hill, New York (1968).
3. H. W. Liepmann, Investigation of laminar boundary layer stability and transition on curved boundaries, NACA Wartime Rep. No. W-107 (1943).
4. H. W. Liepmann, Investigation of boundary layer transition on concave walls, NACA Wartime Rep. No. W-87 (1945).
5. N. Gregory and W. S. Walker, The effect on transition of isolated surface excrescences in the boundary layer, Aeron. Res. Coun. Rep. and Mem. No. 2779 (1951).
6. P. D. McCormack, H. Welker and M. Kelleher, Taylor–Goertler vortices and their effect on heat transfer, *J. Heat Transfer* **92**, 101–112 (1970).
7. W. R. Dean, Fluid motion in a curved channel. *Proc. R. Soc.* **A121**, 402–420 (1928).
8. C. S. Yih and W. M. Sangster, Stability of laminar flows in curved channels, *Phil. Mag. Ser.* 8, **2**, 305–310 (1957).
9. G. Hämmerlin, Die Stabilität der Strömung in einer gekrümmten Kanal, *Archs Ration. Mech. Analysis* **1**, 212–224 (1958).
10. W. H. Reid, On the stability of viscous flow in a curved channel, *Proc. R. Soc.* **A244**, 186–198 (1958).
11. D. B. Brewster, P. Grosberg and A. H. Nissan, The stability of viscous flow between horizontal concentric cylinders, *Proc. R. Soc.* **A251**, 76–91 (1959).
12. S. Chandrasekhar, *Hydrodynamic and Hydromagnetic Stability*. Oxford, London (1961).
13. E. M. Sparrow, On the onset of flow instability in a curved channel of arbitrary height, *Z. Angew. Math. Phys.* **15**, 638–642 (1964).
14. J. Kestin, Discussion of the paper—effects of free stream turbulence and pressure gradient on flat plate boundary layer velocity profiles and on heat transfer, *J. Heat Transfer* **89**, 175–176 (1967).
15. L. Goldstein, Jr., Local mass transfer in corrugated-walled ducts and heat exchanger configurations, Ph.D. Thesis, Department of Mechanical Engineering, University of Minnesota (1975).
16. L. Goldstein, Jr. and E. M. Sparrow, Heat/mass transfer characteristics for flow in a corrugated wall channel, *J. Heat Transfer*. To be published.